



A reaction diffusion model for competing pioneer and climax species  
by Sharon Lynn Brown

A thesis submitted in partial fulfillment of the requirements for the degree of Doctor of Philosophy in  
Mathematics

Montana State University

© Copyright by Sharon Lynn Brown (1998)

Abstract:

Presented is a reaction-diffusion model for the interaction of a pioneer and climax species. The linear stability analysis of the kinetic equilibria are examined and the existence of a Hopf bifurcation is shown. A specific model is used to demonstrate the dynamics of the system. Diffusion is introduced into the kinetic system to model the spatial dispersion of the species. An analysis for the existence of a Turing bifurcation is performed. Again a specific model is examined for the possibility of Turing bifurcations and bifurcation diagrams are produced. Finally traveling wave solutions for the full reaction-diffusion system are examined. It is found using geometric singular perturbation theory that there exists a traveling wave solution to the system with wave speed of  $O(\epsilon)$ .

A REACTION DIFFUSION MODEL  
FOR COMPETING PIONEER AND CLIMAX SPECIES

by

Sharon Lynn Brown

A thesis submitted in partial fulfillment  
of the requirements for the degree

of

Doctor of Philosophy

in

Mathematics

MONTANA STATE UNIVERSITY  
Bozeman, Montana

November 1998

D378  
B8152

APPROVAL

of a thesis submitted by

Sharon Lynn Brown

This thesis has been read by each member of the thesis committee and has been found to be satisfactory regarding content, English usage, format, citations, bibliographic style, and consistency, and is ready for submission to the College of Graduate Studies.

11/20/98  
Date

Jack D. Dockery  
Jack D. Dockery  
Chairperson, Graduate Committee

Approved for the Major Department

11/20/98  
Date

John Lund  
John Lund  
Head, Mathematical Sciences

Approved for the College of Graduate Studies

11/23/98  
Date

Joseph J. Fedock  
Joseph J. Fedock  
Graduate Dean

## STATEMENT OF PERMISSION TO USE

In presenting this thesis in partial fulfillment for a doctoral degree at Montana State University, I agree that the Library shall make it available to borrowers under rules of the Library. I further agree that copying of this thesis is allowable only for scholarly purposes, consistent with "fair use" as prescribed in the U. S. Copyright Law. Requests for extensive copying or reproduction of this thesis should be referred to University Microfilms International, 300 North Zeeb Road, Ann Arbor, Michigan 48106, to whom I have granted "the exclusive right to reproduce and distribute copies of the dissertation for sale in and from microform or electronic format, along with the right to reproduce and distribute my abstract in any format in whole or in part."

Signature Sharon L. Brown

Date 11-16-98

## ACKNOWLEDGEMENTS

I would like to thank both Jack Dockery and Mark Pernarowski for their patience and guidance throughout my time in Montana. I truly appreciate all their help and suggestions along the way. I would also like to thank Joe Raquepas and Kyle Riley for their friendship during these last few years of writing. Finally I would like to thank my family for believing in me and standing behind me throughout this whole process. Thank you Mom, Cathy, Patty, Larry, Jim and Michael. I couldn't have done this without you. I dedicate this thesis to my father, Robert Bruce Brown, I wish you could have been here to celebrate with me.

## TABLE OF CONTENTS

	Page
LIST OF TABLES . . . . .	vi
LIST OF FIGURES . . . . .	vii
ABSTRACT . . . . .	ix
1. Introduction . . . . .	1
2. Kinetic Model Equations . . . . .	5
Equilibria and Stability . . . . .	6
Hopf Bifurcation . . . . .	9
Selgrade Model . . . . .	12
3. Introduction of Diffusion . . . . .	19
Stability of Uniform Steady States . . . . .	22
Analytical Bifurcation Analysis . . . . .	25
Local Bifurcation Analysis of Bifurcating Solutions near $q_1$ . . . . .	26
Selgrade Model with Diffusion . . . . .	31
4. Traveling Waves . . . . .	39
Traveling Waves Along an Axis . . . . .	41
Traveling Waves Along the $U$ Axis . . . . .	41
Traveling Waves Along the $V$ Axis . . . . .	48
Traveling Wave Between the Axis . . . . .	58
Matched asymptotic expansion . . . . .	61
Geometric Singular Perturbation . . . . .	76
5. Conclusion . . . . .	90
REFERENCES CITED . . . . .	95

LIST OF TABLES

Table		Page
1	Equilibria of the Kinetic System . . . . .	9

## LIST OF FIGURES

Figure		Page
1	Pioneer Species Fitness Function, $f$ . . . . .	13
2	Climax Species Fitness Function, $g$ . . . . .	14
3	Pioneer and Climax Nullclines . . . . .	15
4	Hopf Bifurcation Diagram for the Pioneer Species, $u$ . . . . .	16
5	Stability Region for Periodic Solutions Resulting from Hopf Bifurcation. The dotted line is the $a = 0$ curve, the solid line is the $\det(C) = 0$ curve and the dot-dash-dot line is the $\text{tr}(DF(q_1)) = 0$ curve. . . . .	17
6	Graph of $d_2 = 0$ and $d_2$ undefined. . . . .	34
7	Graph of $d_2$ versus $\gamma$ for $c_{11} = 0.25$ . . . . .	35
8	Bifurcation diagram for $c_{11} = 0.25$ , $\gamma = 320$ . . . . .	36
9	Bifurcation diagram for $c_{11} = 0.25$ , $\gamma = 240$ . . . . .	36
10	Graph of $\lambda_m$ versus $m$ for $c_{11} = .25$ , $\gamma = 240$ and $d = d_1^*$ . . . . .	37
11	Graph of $\lambda_m$ versus $m$ for $c_{11} = .25$ , $\gamma = 320$ and $d = d_1^*$ . . . . .	38
12	Bifurcation Diagram for $c_{11} = .25$ and $\gamma = 320$ , mode two solutions are shown with dashed line, mode one solutions with solid line. . . . .	38
13	Traveling Waves in stationary and moving descriptions. . . . .	40
14	$\tilde{f}(u)$ . . . . .	42
15	The phase plane for traveling wave solutions with triangle OPQ. . . . .	44
16	Phase plane portrait of connecting trajectory from $\frac{z_1}{c_{11}}$ to 0 with wave speed $c \geq \sqrt{4D_1\tilde{f}'(0)}$ . Calculated for the Selgrade model with $c_{11} = 0.25$ , $c = 3$ , $D_1 = 1$ . . . . .	47
17	Example of Traveling wave front for the Pioneer species connecting $\frac{z_1}{c_{11}}$ to 0. The wave is moving to the right over time. Selgrade model with $c_{11} = 0.2$ , $D_1 = 1$ . . . . .	48
18	$\tilde{g}(v)$ . . . . .	49
19	Phase plane portrait for climax species $T(c)$ depicts the connecting trajectory corresponding to the traveling wave solution from 0 to $\frac{w_2}{c_{22}}$ for the PDE system. Calculated for Selgrade model with $c_{22} = 1$ , $D_2 = 1$ , $c = 0.33228$ . . . . .	51
20	Eigenvectors at $(0, 0)$ . For $c_1 < c_2$ , $T(c_1) > T(c_2)$ . . . . .	53
21	Eigenvectors at $(\frac{w_2}{c_{22}}, 0)$ . For $c_1 < c_2$ , $T(c_1) < T(c_2)$ , when $0 < V < \frac{w_2}{c_{22}}$ . . . . .	54
22	Trajectories for the system, where $T_1$ is the unstable manifold for the ODE system and $T_2$ is the unstable manifold for the linear ODE system. . . . .	55
23	Level sets of the Hamiltonian for the ODE system. Calculated for the Selgrade model with $c_{22} = 1$ , $D_2 = 1$ . . . . .	57

24	Traveling wave example for traveling wave along v-axis. The wave moves to the left in time. Calculated for the Selgrade model with $c_{22} = 1, D_2 = 1$ . . . . .	58
25	U-V Phase plane diagram of Traveling wave solutions to the full system. Calculated for Selgrade model with $c_{11} = 0.109, c_{22} = 1$ . . . . .	60
26	Wave solutions of Pioneer and Climax species from $(\frac{z_1}{c_{11}}, 0)$ to $(0, \frac{w_2}{c_{22}})$ . Calculated for Selgrade model with $c_{11} = 0.109, c_{22} = 1$ . . . . .	61
27	Phase plane portrait for the first order system with $Y_{10}^+$ . Calculated for the Selgrade model with $c_{11} = 0.2, c_{22} = 1$ . . . . .	65
28	Phase plane portrait for the first order system with $Y_{10}^-$ . Calculated for Selgrade model with $c_{11} = 0.2; c_{22} = 1$ . . . . .	67
29	Combined Phase portrait of the two portions of the outer Pioneer solution. Calculated for the Selgrade model with $c_{11} = 0.2, c_{22} = 1$ . . .	68
30	Saddle-saddle phase plane connections for inner problem with $0 < U^* < w_1$ . . . . .	73
31	Node-saddle connection for inner problem with $w_1 < U^* < w_2$ . . . . .	74
32	Heteroclinic orbit connecting equilibria $(\frac{z_1}{c_{11}}, 0, 0, 0)$ and $(0, 0, \frac{w_2}{c_{22}}, 0)$ . . .	82
33	Slow Manifolds $\mathcal{M}^-$ and $\mathcal{M}^+$ with $P^-(u)$ and $P^+(u)$ . . . . .	83
34	Pioneer and Climax solutions showing complex behavior with $c_{11} = 0.112, D_1 = .001, D_2 = .01$ and initial conditions started near $q_2$ . Numerics done for Selgrade model, $c_{22} = 1$ . Dashed line represents the Pioneer species, solid line represents the Climax species. . . . .	92
35	Pioneer and Climax solutions showing complex behavior with $c_{11} = 0.112, D_1 = .001, D_2 = .01$ and initial conditions started near $q_2$ . Complex behavior taken over by traveling wave front moving to $(0, \frac{w_2}{c_{22}})$ steady state. Numerics done for Selgrade model, $c_{22} = 1$ . Dashed lines represent Pioneer species, solid line represents the Climax species. The wave front is moving from the left to the right. . . . .	92
36	Pioneer and Climax solutions showing complex behavior with $c_{11} = 0.118, D_1 = .001, D_2 = .01$ and initial conditions started near $q_2$ . This behavior appears to persist. Numerics done for Selgrade model, $c_{22} = 1$ . Dashed lines represent Pioneer species, solid lines represent Climax species. . . . .	93

**ABSTRACT**

Presented is a reaction-diffusion model for the interaction of a pioneer and climax species. The linear stability analysis of the kinetic equilibria are examined and the existence of a Hopf bifurcation is shown. A specific model is used to demonstrate the dynamics of the system. Diffusion is introduced into the kinetic system to model the spatial dispersion of the species. An analysis for the existence of a Turing bifurcation is performed. Again a specific model is examined for the possibility of Turing bifurcations and bifurcation diagrams are produced. Finally traveling wave solutions for the full reaction-diffusion system are examined. It is found using geometric singular perturbation theory that there exists a traveling wave solution to the system with wave speed of  $O(\epsilon)$ .

## CHAPTER 1

**Introduction**

In an ecosystem, the competition among plant or animal species for natural resources is important in determining the evolution of the system. For example each tree in a forest competes with its neighbors for light, space, carbon dioxide, and soil nutrients. Although the intensity of the competition may or may not be affected by the species type of the neighboring trees, it is affected by neighboring population density. Similarly an animal may not be affected by what type of competitor is consuming its food, but the amount of food available will be affected by the density of the competitor population. We try to model the effects of population density on the survival and growth of an individual species by assuming that the species' per capita growth rate (i.e., fitness) is a function of a weighted total density variable. This total density variable is a linear combination of the densities of the interacting species with coefficients weighting the intensity of the effect of each species, both the intra-specific and inter-specific species competition. The intra-specific competition describes the extent by which each individual within a population affects and is affected by the other individuals within that particular population. Inter-specific competition describes the effects on individuals due to a species of a differing population. In both cases these effects may be either positive or negative. See [15] for examples of both intra and inter-specific competition. An example of such a model is the Lotka-Volterra system where the per capita growth rate is just a linear combination of the densities of the interacting populations [18].

Typically a fitness function will possess certain monotonicity properties as a function of it's density. We would expect that for large enough values of the density

variable, corresponding to crowding, the fitness of a species should decrease. For example, certain varieties of pine and poplar have higher fitnesses at low density but have fitnesses which decrease with an increase in the density of the surrounding forest. In a forest ecosystem, a tree population whose fitness monotonically decreases with density is called a pioneer species. We adopt that terminology here. An example of such functions can be seen in the Lotka-Volterra system where the fitness,  $f_i$ , of a pioneer species is linear:

$$f_i(y_i) = r_i - y_i, \quad (1.1)$$

with  $y_i = \sum_{j=1}^n c_{ij}x_j$  representing the weighted total density variable for the  $i^{\text{th}}$  population and  $x_j$  represents the population density of the  $j^{\text{th}}$  population. It has been suggested by Ricker, [21], that certain fish populations have exponential pioneer fitnesses of the form (see Figure 1)

$$f(y) = e^{r(1-y)} - a. \quad (1.2)$$

Hassell and Comins [10] studied a two-species competition model with a pioneer fitness of the form

$$f(y) = \frac{r}{(1 + by)^p} - a. \quad (1.3)$$

Certainly not all species fall into the category of a pioneer. For many species their survival and reproduction rates will benefit from an increase in density, at least for a period of time. Things such as group defense for prey, increased gene pool, and enhanced soil nutrients can represent the benefits of a higher density. An example of such species are oak or maple trees. At intermediate densities these species benefit from the presence of additional trees which provide protection and improved soil conditions; but ultimately individual reproduction and survival decrease at increasingly higher densities. We refer to such a species as a climax species. Its fitness will mono-

tonically increase to a maximum value and then monotonically decrease as a function of the weighted total density. Cushing [2] in his analysis of age-structured populations and Selgrade and Namkoong [23, 24, 22] for a forest model suggest climax fitnesses in the form (see Figure 2)

$$f(y) = ye^{r(1-y)} - a. \quad (1.4)$$

In this thesis we will analyze a two dimensional system of differential equations which model the interaction between a pioneer species and a climax species. In Chapter 2 we analyze the kinetic interaction model. The chapter is a review of results presented in [23, 24, 22] along with analyses of a specific example, referred to as the Selgrade model. We present local stability results for the equilibria of the general model using linear stability analysis. Results for the Selgrade model showing the existence and stability of bifurcating periodic solutions originating from a Hopf bifurcation of an interior equilibrium point are presented. For this specific model we show that the periodic solutions are stable.

In Chapter 3, we consider a model for interacting pioneer and climax species with the addition of a spatial variable in a diffusion term, modeling the spatial movement of the species. Only one spatial dimension is introduced. We again analyze the stability of the spatially homogeneous equilibria found in Chapter 2. The analysis of the bifurcation of these steady states is performed with local analysis of the shape of the bifurcation diagram. Again the specific example introduced in Chapter 2, Selgrade's model, is examined in detail. Numerical results suggest that the initial mode to bifurcate need not be a mode one solution of the form  $a \cos(\pi x)$ , and because of this the stability of the bifurcating solutions are not determined. We present numerical results showing that the bifurcation diagram near the critical point could open to the right or the left depending on the parameters space. We also give numerical evidence that for some range of the parameter space the higher order modes bifurcate

prior to the first mode as a certain bifurcating parameter is increased.

In Chapter 4, traveling wave solutions to the model are examined. First traveling waves in the absence of one species are determined. We show the existence of traveling waves for each species in the absence of the other. Next we analyze the existence of a traveling wave with  $O(\epsilon)$  wave speed. This is an invasive wave connecting the equilibria along the opposing axes. An approximate solution is found using methods of matched asymptotic expansions. Next we show using geometric singular perturbation theory the existence of the traveling wave for small wave speed that is near the approximate solution.

## CHAPTER 2

## Kinetic Model Equations

In this chapter we will analyze a two dimensional system of differential equations which models the interaction between a pioneer species and a climax species. We let  $u$  denote the density of the pioneer species with its fitness function,  $f$ , being a monotonically decreasing function having only one positive zero. The climax species density we represent as  $v$ . Its fitness function,  $g$ , will increase to a maximum and then decrease, having exactly two positive zeros. See Figures 1 and 2 for examples of pioneer and climax species fitness functions respectively.

Both fitnesses will be taken to depend on total density variables,  $y_i$ , defined as a linear combination of the population densities. We define them as

$$y_1 = c_{11}u + c_{12}v, \quad (2.1)$$

$$y_2 = c_{21}u + c_{22}v, \quad (2.2)$$

where  $c_{ij} \geq 0$  is an interaction coefficient which weights the effect of the  $j^{\text{th}}$  population on the  $i^{\text{th}}$  population. The coefficients  $c_{11}$  and  $c_{22}$  pertain to intra-species interaction, and  $c_{12}$  and  $c_{21}$  refer to inter-species interaction.

The model equations for this system of interacting pioneer and climax species are given by,

$$\begin{aligned} \frac{du}{dt} &= uf(y_1), \\ \frac{dv}{dt} &= vg(y_2). \end{aligned} \quad (2.3)$$

In vector form, (2.3) may be written as

$$\frac{d\vec{u}}{dt} = \mathbf{F}(\vec{u}). \quad (2.4)$$

This vector field is defined on the positive cone in  $\mathbb{R}^2$ . By restricting  $c_{12} \neq 0$  and  $c_{21} \neq 0$  and rescaling  $y_1$  and  $y_2$  we may assume that  $c_{12}$  and  $c_{21}$  are equal to one. Thus, without loss of generality we let  $c_{12} = c_{21} = 1$  throughout. Then interaction matrix  $C$  becomes;

$$C = \begin{pmatrix} c_{11} & 1 \\ 1 & c_{22} \end{pmatrix}. \quad (2.5)$$

In the first section the equilibria of system (2.3) along with their stability are discussed. In the following section we show the existence of a Hopf bifurcation. Finally in the third section a specific example of system (2.3), which will be used throughout the thesis is examined.

### Equilibria and Stability

Equilibria of system (2.3) occur where the nullclines of the pioneer species intersect the nullclines of the climax species. Let  $z_1 > 0$  be the zero of  $f$ . Then the  $u$ -nullclines for system (1) are given by

$$u = 0 \text{ and } z_1 = c_{11}u + v. \quad (2.6)$$

We assume that  $z_1$  is a non-degenerate zero of  $f$ , and indeed we assume  $f'(z_1) < 0$ .

Let  $w_1$  and  $w_2$  denote the zeros of  $g$ , with  $0 < w_1 < w_2$ ,  $g'(w_1) > 0$ , and  $g'(w_2) < 0$ . The  $v$ -nullclines are

$$v = 0, \quad w_1 = u + c_{22}v, \quad \text{and} \quad w_2 = u + c_{22}v. \quad (2.7)$$

Notice that all the nullclines are straight lines and that two of the  $v$ -nullclines associated with the zeros of  $g$  are parallel. In Figure (3) we indicate a typical plot of these nullclines noting that slopes and equilibria location depend on  $c_{11}$ ,  $c_{22}$  and the specific model.

There are six equilibrium points for this system, four of which always occur on the axes. The equilibria along the axes are

$$p_0 = (0, 0), \quad p_1 = \left(0, \frac{w_1}{c_{22}}\right), \quad p_2 = \left(0, \frac{w_2}{c_{22}}\right), \quad p_3 = \left(\frac{z_1}{c_{11}}, 0\right). \quad (2.8)$$

These points correspond to one of the species being extinct or, in the case of  $p_0$ , both being extinct. The other equilibria are

$$q_i = \left(\frac{c_{22}z_1 - w_i}{\det(C)}, \frac{c_{11}w_i - z_1}{\det(C)}\right) = (u_i^*, v_i^*), \quad i = 1, 2, \quad (2.9)$$

where  $\det(C)$  is the determinant of the interaction coefficient matrix (2.5). Lastly we note that to be of biological significance, it is necessary for both components of the equilibria to be nonnegative.

To determine the stability of the equilibria, we first find the eigenvalues of the Jacobian of the vector field at each of these points. The Jacobian can be expressed in the following form:

$$DF(\vec{u}) = \begin{pmatrix} f(y_1) & 0 \\ 0 & g(y_2) \end{pmatrix} + \begin{pmatrix} uf'(y_1) & 0 \\ 0 & vg'(y_2) \end{pmatrix} \begin{pmatrix} c_{11} & 1 \\ 1 & c_{22} \end{pmatrix}.$$

For the equilibrium point  $p_0$  given in (2.8),

$$DF(p_0) = \begin{pmatrix} f(0) & 0 \\ 0 & g(0) \end{pmatrix}. \quad (2.10)$$

The eigenvalues are given by  $\lambda_1 = f(0)$  and  $\lambda_2 = g(0)$ . Since we assume the fitness functions satisfy  $f(0) > 0$  and  $g(0) < 0$  it follows that  $p_0$  is a saddle.

The next two equilibria from equation (2.8),  $p_{1,2}$ , can be examined simultaneously. The Jacobian for these points is given by

$$DF(p_{1,2}) = \begin{pmatrix} f\left(\frac{w_{1,2}}{c_{22}}\right) & 0 \\ \frac{w_{1,2}}{c_{22}}g'(w_{1,2}) & w_{1,2}g'(w_{1,2}) \end{pmatrix}. \quad (2.11)$$

The eigenvalues of  $DF(p_{1,2})$  are  $\lambda_1 = f\left(\frac{w_{1,2}}{c_{22}}\right)$  and  $\lambda_2 = w_{1,2}g'(w_{1,2})$ . Recall that  $g'(w_1) > 0$  and  $g'(w_2) < 0$ , therefore  $\lambda_2$  is positive for  $p_1$  and is negative for  $p_2$ . The

sign of  $\lambda_1$  is determined by  $f(\frac{w_{1,2}}{c_{22}})$ , which can either be positive or negative. If  $\lambda_1$  is negative then  $p_1$  is a saddle and  $p_2$  is a sink. However, if  $\lambda_1$  is positive then  $p_1$  is a source and  $p_2$  is a saddle.

Evaluating the Jacobian at the equilibrium  $p_3$  stated in equation (2.8) gives,

$$DF(p_3) = \begin{pmatrix} z_1 f'(z_1) & \frac{z_1}{c_{11}} f'(z_1) \\ 0 & g(\frac{z_1}{c_{11}}) \end{pmatrix}. \quad (2.12)$$

Here the eigenvalues are  $\lambda_1 = z_1 f'(z_1)$  and  $\lambda_2 = g(\frac{z_1}{c_{11}})$ . Since  $f'(z_1) < 0$  it follows that  $\lambda_1 < 0$ . On the other hand  $\lambda_2$  can change sign depending on the value of  $g(\frac{z_1}{c_{11}})$ . For  $p_3$  between the two  $u$ -intercepts of the  $v$ -nullclines corresponding to  $g = 0$  (see Figure 3),  $\lambda_2 = g(\frac{z_1}{c_{11}}) > 0$ , so  $p_3$  is a saddle, otherwise  $p_3$  is stable.

Lastly we consider the equilibria off the axes,  $q_1$  and  $q_2$ . From (2.9) we find

$$DF(q_i) = \begin{pmatrix} c_{11} u_i^* f'(z_1) & u_i^* f'(z_1) \\ v_i^* g'(w_i) & c_{22} v_i^* g'(w_i) \end{pmatrix}. \quad (2.13)$$

The characteristic equation is given by

$$\lambda^2 - \text{tr}(DF(q_i))\lambda + \det(DF(q_i)) = 0$$

where

$$\text{tr}(DF(q_i)) = c_{11} u_i^* f'(z_1) + c_{22} v_i^* g'(w_i), \quad (2.14)$$

$$\det(DF(q_i)) = u_i^* v_i^* f'(z_1) g'(w_i) \det(C). \quad (2.15)$$

The eigenvalues are given by

$$\lambda_{\pm} = \frac{\text{tr}(DF(q_i)) \pm \sqrt{(\text{tr}(DF(q_i)))^2 - 4\det(DF(q_i))}}{2}. \quad (2.16)$$

We look first at the equilibrium  $q_2$ . Since  $f'(z_1) < 0$  and  $g'(w_2) < 0$  it follows from (2.14) that  $\text{tr}(DF(q_2)) < 0$ . The sign of  $\det(DF(q_2))$  depends on  $\det(C)$ . If  $\det(C) < 0$  then  $\det(DF(q_2)) < 0$  and the eigenvalues are real and of opposite sign,

thus  $q_2$  is a saddle point. If  $\det(C) > 0$  then  $\det(DF(q_2)) > 0$  but,  $\text{Re}(\lambda_{\pm})$  will remain less than zero so in this case  $q_2$  is a stable equilibrium.

Finally consider the equilibrium  $q_1$ . Here  $\text{tr}(DF(q_1))$  may be positive, negative or zero. However, if  $\det(C) > 0$  then, since  $f'(z_1) < 0$  and  $g'(w_1) > 0$  it follows by (2.15) that  $\det(DF(q_1)) < 0$ . Thus both eigenvalues are real, and of opposite sign, making  $q_1$  a saddle. On the other hand if  $\det(C) < 0$  then the eigenvalues of  $DF(q_1)$  have real parts with the same sign. In this case if  $\text{tr}(DF(q_1)) < 0$  the  $q_1$  is locally asymptotically stable, and if  $\text{tr}(DF(q_1)) > 0$  then  $q_1$  is unstable. In the next section we show that by varying either  $c_{11}$  or  $c_{22}$ ,  $q_1$  may undergo a Hopf bifurcation yielding a periodic orbit.

We summarize the stability of the equilibria for system (2.3) in Table 1 below.

Table 1: Equilibria of the Kinetic System

point	condition	stability
$p_0 = (0, 0)$	none	saddle
$p_1 = (0, \frac{w_1}{c_{22}})$	$f(\frac{w_2}{c_{22}}) < 0$	saddle
	$f(\frac{w_2}{c_{22}}) > 0$	unstable
$p_2 = (0, \frac{w_2}{c_{22}})$	$f(\frac{w_2}{c_{22}}) < 0$	stable
	$f(\frac{w_2}{c_{22}}) > 0$	saddle
$p_3 = (\frac{z_1}{c_{11}}, 0)$	$g(\frac{z_1}{c_{11}}) < 0$	stable
	$g(\frac{z_1}{c_{11}}) > 0$	saddle
$q_1 = (\frac{c_{22}z_1 - w_1}{\det C}, \frac{c_{11}w_1 - z_1}{\det C})$	$\det C > 0$	saddle
	$\det C < 0$ and $\text{tr}(DF(q_1)) < 0$	stable
	$\det C < 0$ and $\text{tr}(DF(q_1)) > 0$	unstable
$q_2 = (\frac{c_{22}z_1 - w_2}{\det C}, \frac{c_{11}w_2 - z_1}{\det C})$	$\det C > 0$	stable
	$\det C < 0$	saddle

## Hopf Bifurcation

In this section we show that the equilibrium  $q_1$  may undergo a Hopf bifurcation as we

vary  $c_{11}$  or  $c_{22}$ . In general, for a Hopf bifurcation to occur as a parameter changes, complex eigenvalues of the Jacobian at the equilibrium point must cross the imaginary axis. This crossing results in a change of the stability of the equilibrium point and often gives rise to periodic solutions. From equation (2.16) we see that for  $DF(q_1)$  to have complex eigenvalues we need

$$(tr(DF(q_1)))^2 < 4det(DF(q_1)).$$

The inequality implies that  $det(DF(q_1))$  must be greater than zero, and so by (2.15) with  $g'(w_1) > 0$ ,  $f'(z_1) < 0$  we have that  $det(C)$  must be less than zero. By choosing parameter values such that  $tr(DF(q_1)) = 0$  we get purely imaginary eigenvalues for the Jacobian at  $q_1$ . In equation (2.14) we see that by varying  $c_{11}$  or  $c_{22}$  we can make  $tr(DF(q_1)) = 0$ . Thus, we can choose either  $c_{11}$  or  $c_{22}$  as the bifurcation parameter. Biologically, adjusting these parameters would be equivalent to the stocking or harvesting of one particular species or, amplifying or diminishing the intra-species competition.

Setting  $tr(DF(q_1)) = 0$  and solving for  $c_{11}$  gives

$$c_{11} = \frac{c_{22}z_1g'(w_1)}{(c_{22}z_1 - w_1)f'(z_1) + c_{22}w_1g'(w_1)} \quad (2.17)$$

or  $c_{22}$ ,

$$c_{22} = \frac{c_{11}w_1f'(z_1)}{(c_{11}w_1 - z_1)g'(w_1) + c_{11}z_1f'(z_1)}. \quad (2.18)$$

Let  $c_{11}^*$  and  $c_{22}^*$  denote these respective values. To ensure that  $u_1^*$  and  $v_1^*$  are positive, making  $q_1$  biologically significant, we need

$$c_{22}z_1 - w_1 < 0 \text{ and } c_{11}w_1 - z_1 < 0. \quad (2.19)$$

These inequalities also imply both  $c_{11}^*$  and  $c_{22}^*$  are positive.

Having purely imaginary eigenvalues is not enough to produce a Hopf bifurcation. We also need the eigenvalues to cross the imaginary axis transversality as

the bifurcation parameter is varied. This amounts to the real part of the eigenvalues having a nonzero derivative with respect to the parameter at the critical value of the bifurcation parameter (i.e. at  $c_{11}^*$  or  $c_{22}^*$ ). If we have complex eigenvalues, we see from equation (2.16) that the real part of the eigenvalues are

$$\begin{aligned}\alpha(c_{ii}) &= \frac{1}{2} \text{tr}(DF(q_1(c_{ii}), c_{ii})), \\ &= \frac{1}{2} \frac{[(c_{22}z_1 - w_1)c_{11}f'(z_1) + (c_{11}w_1 - z_1)c_{22}g'(w_1)]}{\det(C)}.\end{aligned}$$

Choosing  $c_{11}$  as the bifurcation parameter and fixing  $c_{22}$  gives

$$\alpha'(c_{11}^*) = \frac{1}{2} \frac{(c_{22}z_1 - w_1)f'(z_1) + c_{22}w_1g'(w_1)}{\det(C)}.$$

Therefore with the first inequality of (2.19) we see that  $\alpha'(c_{11}^*) < 0$ . Thus, as  $c_{11}$  decreases through  $c_{11}^*$  the fixed point  $q_1$  destabilizes and a periodic solution bifurcates.

Letting  $c_{22}$  be the bifurcating parameter and fixing  $c_{11}$  gives

$$\alpha'(c_{22}^*) = \frac{1}{2} \frac{(c_{11}w_1 - z_1)g'(w_1) + c_{11}z_1f'(z_1)}{\det(C)},$$

and using (2.19) again, this implies  $\alpha'(c_{22}^*) > 0$ . Therefore,  $q_1$  stabilizes with periodic solutions bifurcating as  $c_{22}$  increases past  $c_{22}^*$ .

We can summarize the above by stating that a Hopf bifurcation occurs at  $q_1$  with respect to the parameter  $c_{11}$  as  $c_{11}$  decreases through  $c_{11}^*$ . Likewise a Hopf bifurcation occurs with respect to  $c_{22}$  as  $c_{22}$  increases through  $c_{22}^*$ .

The following theorem [9] can be used to determine the stability of the bifurcating periodic solution arising from the Hopf bifurcation of  $q_1$  at  $c_{11}^*$  or  $c_{22}^*$ .

**Theorem 2.1** *Suppose that the system  $\frac{d\vec{x}}{dt} = \vec{h}_\mu(\vec{x}) = \begin{bmatrix} h_\mu(\vec{x}) \\ k_\mu(\vec{x}) \end{bmatrix}$ ,  $\vec{x} \in \mathbb{R}^2$ ,  $\mu \in \mathbb{R}$  has an equilibrium  $(\vec{x}_0, \mu_0)$  at which a Hopf bifurcation occurs. Let*

$$\frac{d}{d\mu}(\text{Re}(\lambda(\mu)))|_{\mu=\mu_0} = d \neq 0,$$

where  $\lambda(\mu)$  and  $\bar{\lambda}(\mu)$  are the eigenvalues of the linearized system. Then there is a three-dimensional center manifold passing through  $(\bar{x}_0, \mu_0)$  in  $\mathbb{R}^2 \times \mathbb{R}$  and a smooth system of coordinates for which the Taylor expansion of degree 3 on the center manifold is given by the following;

$$\begin{aligned} \dot{x} &= (d\mu + a(x^2 + y^2))x - (\omega + c\mu + b(x^2 + y^2))y \\ \dot{y} &= (\omega + c\mu + b(x^2 + y^2))x + (d\mu + a(x^2 + y^2))y, \end{aligned} \quad (2.20)$$

with  $a$  given by

$$\begin{aligned} a &= \frac{1}{16}[h_{xxx} + h_{xyy} + k_{xxy} + k_{yyx}] + \frac{1}{\text{Im}(\lambda(\mu_0))}[h_{xy}(h_{xx} + h_{yy}) \\ &\quad - k_{xy}(k_{xx} + k_{yy}) - h_{xx}k_{xx} + h_{yy}k_{yy}]. \end{aligned} \quad (2.21)$$

If  $a \neq 0$ , there is a surface of periodic solutions in the center manifold which has a quadratic tangency at  $\mu_0$  agreeing to second order with the paraboloid  $\mu = -(\frac{a}{d})(x^2 + y^2)$ . If  $a < 0$ , then these periodic solutions are stable limit cycles, while if  $a > 0$ , the periodic solutions are repelling.

For system (2.3) the stability coefficient  $a$  given in (2.21) at  $q_1$  is given by

$$\begin{aligned} 16a &= \frac{c_{11}^2 w_1 f''(z_1)}{c_{22} v_1^*} + \frac{c_{22} z_1 g''(w_1)}{w_1^*} + c_{11} u_1^* f'(z_1) \det C \left[ \frac{g''}{g'} \right]'(w_1) \\ &\quad + c_{11} v_1^* g'(w_1) \det C \left[ \frac{f''}{f'} \right]'(z_1). \end{aligned} \quad (2.22)$$

In the next section we use (2.22) and Theorem 2.1 to determine the stability of the bifurcated periodic solutions in a specific pioneer-climax model.

### Selgrade Model

In this section, we will analyze the pioneer-climax model introduced in Selgrade [22] and Selgrade and Namkoong [23, 24]. In this model both the pioneer and climax

fitness functions are exponential functions of the total population density. The fitness function for the pioneer species is given by

$$f(y_1) = -1 + \exp(1 - 2y_1), \quad (2.23)$$

with a zero at  $z_1 = \frac{1}{2}$  (see Figure 1).

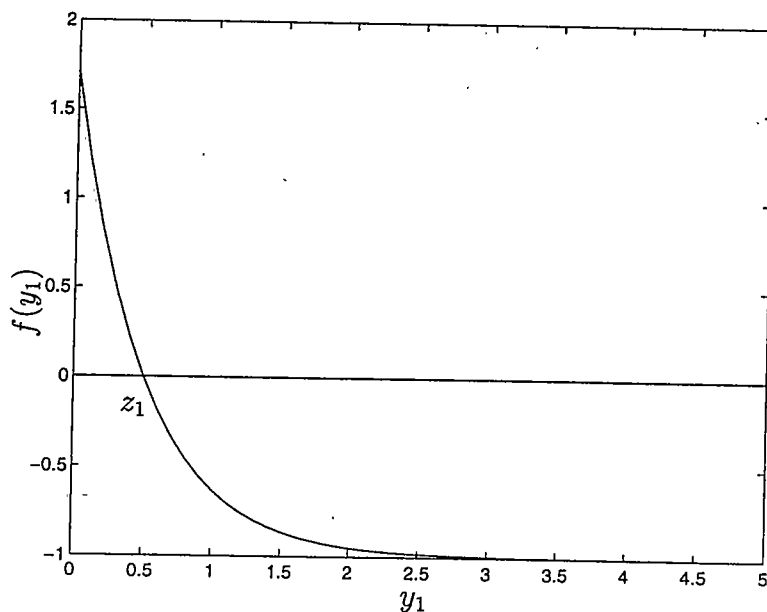


Figure 1: Pioneer Species Fitness Function,  $f$

The climax species' fitness function is given by

$$g(y_2) = -1 + y_2 \exp\left[\frac{1}{2}(1 - y_2)\right], \quad (2.24)$$

and has zeros at  $w_1 = 1$  and  $w_2 \approx 3.513$  (see Figure 2).

For this example we choose  $c_{11} > 0$  as the bifurcation parameter and fix the value of  $c_{22}$  at one. With this in mind, it follows from (2.5) that  $\det(C) = c_{11} - 1$ . As we saw in the first two sections, a Hopf bifurcation for this system will only occur when  $\det(C) < 0$ , therefore we restrict our attention to  $c_{11} \in (0, 1)$ .

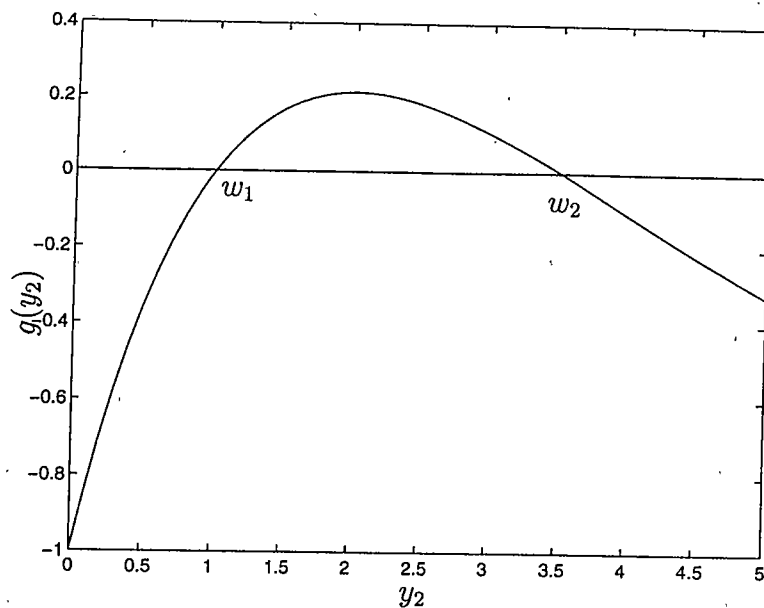


Figure 2: Climax Species Fitness Function,  $g$

In the case of  $c_{22} = 1$ , the  $u$ -nullclines for (2.3) are given by

$$\begin{aligned} u &= 0, \\ v &= \frac{1}{2} - c_{11}u, \end{aligned}$$

and the  $v$ -nullclines are

$$\begin{aligned} v &= 0, \\ v &= 1 - u, \\ v &\approx 3.513 - u. \end{aligned}$$

In Figure 3 we show the nullclines and the equilibria of the system for a typical value of  $c_{11}$ . The equilibria along the axes are given by

$$p_0 = (0, 0), \quad p_1 = (0, 1), \quad p_2 \approx (0, 3.513) \quad \text{and} \quad p_3 = \left(\frac{1}{c_{11}}, 0\right). \quad (2.25)$$

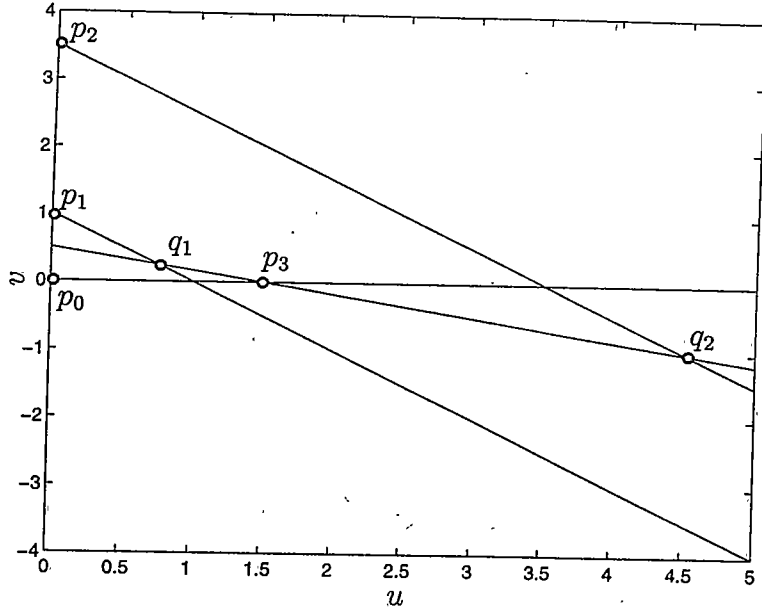


Figure 3: Pioneer and Climax Nullclines

The equilibria interior to the positive cone are

$$q_1 = \left( \frac{1}{2(1-c_{11})}, \frac{1-2c_{11}}{2(1-c_{11})} \right) \text{ and } q_2 \approx \left( \frac{6.02}{2(1-c_{11})}, \frac{1-7.02c_{11}}{2(1-c_{11})} \right). \quad (2.26)$$

From the general stability results presented in Section 1 we can easily determine the stability of the fixed points for this model. We see from Table 1 that the stability for a number of the fixed points is not dependent on  $c_{11}$ . Notice that both  $p_0$  and  $p_1$  are always unstable and since  $f(w_2) < 0$  it follows that  $p_2$  is stable. The last equilibrium whose stability does not depend directly on  $c_{11}$  is  $q_2$ . It is unstable when  $\det(C) < 0$ . From Table 1 we see that the stability of  $p_3$  and  $q_1$  depend on  $c_{11}$ .

The stability of  $p_3$  varies with the sign of  $g(\frac{1}{c_{11}})$ . If  $g(\frac{1}{c_{11}}) < 0$  then  $p_3$  is a sink and if  $g(\frac{1}{c_{11}}) > 0$  then  $p_3$  is a saddle. In terms of  $c_{11}$ ,  $g(\frac{1}{c_{11}})$  is positive for  $c_{11} > \frac{1}{2}$  or  $c_{11} < \frac{1}{2w_2}$  and  $g(\frac{1}{c_{11}})$  is negative for  $\frac{1}{2w_2} < c_{11} < \frac{1}{2}$ . Thus,  $p_3$  is a sink if  $c_{11} > \frac{1}{2}$  or  $c_{11} < \frac{1}{2w_2}$  and a saddle if  $\frac{1}{2w_2} < c_{11} < \frac{1}{2}$ .

Next we note that the point  $q_1$  undergoes a Hopf bifurcation at  $c_{11} = c_{11}^* = \frac{1}{6}$ .

In particular for  $c_{11} > \frac{1}{6}$ ,  $q_1$  is stable and for  $0 < c_{11} < \frac{1}{6}$ ,  $q_1$  is unstable with a branch of periodic orbits that bifurcate at  $c_{11} = \frac{1}{6}$ . The stability of these periodic orbits is determined by the value of  $a$  given in (2.22). Evaluating (2.22) at  $c_{11}^* = \frac{1}{6}$  for the particular fitness functions under consideration gives  $a < 0$  and therefore the bifurcating periodic orbits are locally asymptotically stable. Thus, the system has a supercritical Hopf bifurcation at  $c_{11} = \frac{1}{6}$ . The local form of the bifurcation diagram are determined by the sign of  $\lambda'(c_{11}^*)$  and  $a$ . With both  $\text{Re}(\lambda'(c_{11}^*)) < 0$ , and  $a < 0$ , locally at  $q_1$  the bifurcation diagram is a parabola that opens to the left, from which it follows that the periodic solutions are locally asymptotically stable. Figure 4 shows the bifurcation diagram for the pioneer species,  $u$ . It was created using xppaut [5] with  $c_{11} = 0.3333$  and initial condition  $u = 0.75$ ,  $v = 0.25$ .

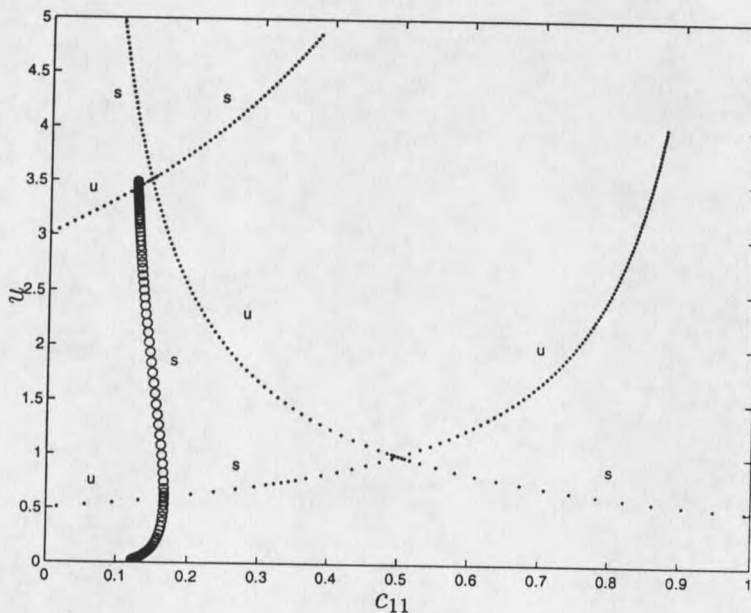


Figure 4: Hopf Bifurcation Diagram for the Pioneer Species,  $u$ .

In general, the analysis done here for  $c_{11}$  as the bifurcation parameter may be duplicated for the case of  $c_{22}$  as the parameter with  $c_{11}$  fixed. The stability diagram

in Figure 5 is for a Hopf bifurcation of  $q_1$  with general  $c_{11}$  and  $c_{22}$  values. In this figure the  $a = 0$  curve was calculated using AUTO [19]. For a Hopf bifurcation to occur at  $q_1$  we need the  $\text{tr}(DF(q_1)) = 0$  and  $\det(C) < 0$ . The stability of the bifurcating periodic orbits depends on the sign of  $a$  at the bifurcating point. In Figure 5  $\det(C) = 0$ ,  $\text{tr}DF(q_1) = 0$  and  $a = 0$  are graphed in the  $(c_{11}, c_{22})$ -plane. Periodic orbits emerge from  $q_1$  for  $(c_{22}, c_{11})$  in the lower region of the graph with  $0 < c_{22} < 2$  on the curve  $\text{tr}DF(q_1) = 0$  and below the graph of  $\det(C) = 0$ . From this we see that the Hopf bifurcation curve,  $\text{tr}DF(q_1) = 0$ , always lies below the  $a = 0$  curve in the region where  $a < 0$ . Thus the bifurcated periodic orbits must be locally asymptotically stable by Theorem 2.1.

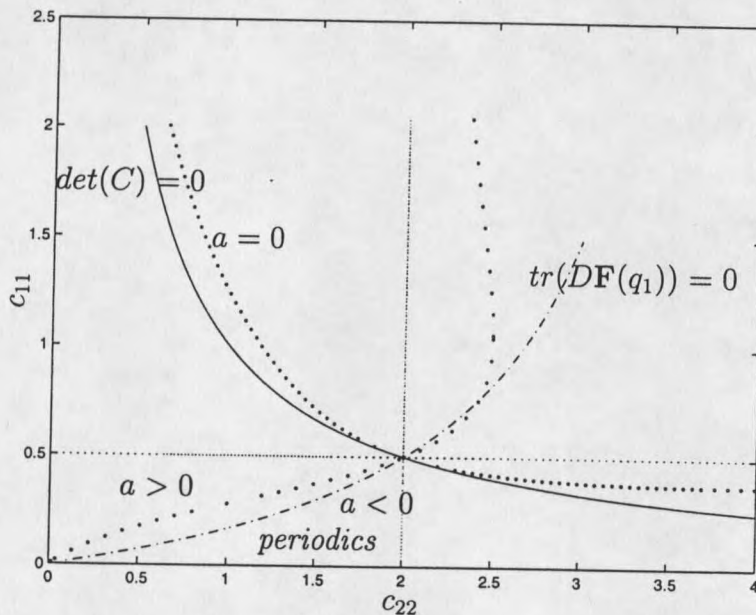


Figure 5: Stability Region for Periodic Solutions Resulting from Hopf Bifurcation. The dotted line is the  $a = 0$  curve, the solid line is the  $\det(C) = 0$  curve and the dot-dash-dot line is the  $\text{tr}(DF(q_1)) = 0$  curve.

For simple models, like the one presented in this chapter, it would seem reasonable that the climax species, being more robust at higher population densities,

would have a greater chance of survival and would eventually exclude the pioneer species as the total density increased. The ultimate dynamical result of an undisturbed pioneer-climax system has been assumed to be the exclusion of the pioneer. However contrary to this belief, our model shows that the densities of both species may fluctuate in a stable periodic fashion for all time. Selgrade and Namkoong [23] argue that the inevitability of a pioneer giving way to a climax species is sometimes an invalid assumption. They give examples of two species usually classified as intolerant pioneers, the *Populus tremuloides* (quaking aspen) in Utah and the *Liriodendron tulipifera* (yellow-popular) in Georgia, that may be evidence of persistence of pioneer species in "climax" communities.

## CHAPTER 3

## Introduction of Diffusion

In this chapter we will introduce a spatial variable into the dynamics of the interacting species model of Chapter 2. In an ecosystem we see that spatial considerations, such as the size of the domain of the species, the conditions along the domain boundary, the concentration of the species throughout and the make-up of the terrain within the domain will affect the existence and survival of a species.<sup>1</sup> We can see that the differences in individual species are partly due to the non-constant environment in which they live, and that the effects of the spatial distribution of the individual species will influence the way they interact. We will see that spatial heterogeneity can have an important effect on the balance that exists between the interaction of differing species. With these spatial effects in mind we will introduce a spatial variable into our pioneer-climax model.

One of the most important sources of collective motion on the molecular level is diffusion, which is a consequence of the perpetual motion of individual molecules. Okubo [17] describes diffusion as the phenomenon by which an organism as a whole spreads due to the irregular motion of each individual. Among the first to draw an analogy between the random motion of molecules and that of organisms was Skellam [27]. He suggested that for a population that is reproducing continuously with rate  $\alpha$  and spreading over space in a random way, a suitable continuous description could be

$$\frac{\partial P}{\partial t} = D\nabla^2 P + \alpha P, \quad (3.1)$$

where  $D$  is called the dispersion rate or the diffusion coefficient and  $P(x, t)$  is the population density. Applying this assumption, Skellam modeled the spread of a muskrat

population over central Europe. Comparing his results with that of actual data he was able to demonstrate that the spread of certain populations can be explained using a diffusion approximation. Since then diffusion models have been used to model the population of a number of species (see [16], [3],[17] and the references therein).

Typically diffusion is thought of as a stabilizing process, something that will have a smoothing or homogenizing influence on the system eventually leading to a uniform spatial distribution. However, in the 1950's Turing suggested that under certain conditions diffusion can act as a destabilizing influence on the system producing steady state solutions that are spatially heterogeneous: "*A reaction diffusion system exhibits diffusion-driven instability or Turing instability if the homogeneous steady state is stable to small perturbations in the absence of diffusion but unstable to small spatial perturbations when diffusion is present*" [16].

We will consider the following system of equations, where  $A(x, t)$  and  $B(x, t)$  represent two species,

$$\begin{aligned} \frac{\partial A}{\partial t} &= F(A, B) + D_A \frac{\partial^2 A}{\partial x^2} \\ \frac{\partial B}{\partial t} &= G(A, B) + D_B \frac{\partial^2 B}{\partial x^2}. \end{aligned} \quad (3.2)$$

Turing's idea is that if in the absence of diffusion (i.e.  $D_A = D_B = 0$ ),  $A$  and  $B$  tend to a linearly stable uniform steady state, then under certain conditions, spatially inhomogeneous patterns can evolve by diffusion driven instability if  $D_A \neq D_B$ . The reaction rates at any given point may not be able to adjust quickly enough to reach equilibrium. If the conditions are right, a small spatial disturbance can become unstable and a pattern begins to grow. Such an instability is said to be diffusion driven and the change in stability due to diffusion is often called a Turing bifurcation.

We will continue to model the interaction of a pioneer species with a climax species but will now introduce diffusion. For simplicity we consider only one spatial

variable and scalar diffusion coefficients. The system of equations are given by,

$$\begin{aligned}u_t &= D_1 u_{xx} + uf(y_1) \\v_t &= D_2 v_{xx} + vg(y_2),\end{aligned}\tag{3.3}$$

with Neumann boundary conditions are given by

$$\begin{aligned}u_x(0, t) &= v_x(0, t) = 0, \\u_x(L, t) &= v_x(L, t) = 0.\end{aligned}\tag{3.4}$$

Neumann boundary conditions impose the condition that the species will not grow or decline due to fluctuations across the boundary of their domain. This may be due to an unfavorable environment outside of their domain such as a change in terrain conditions, lack of water or low food supply. Possibly the boundary conditions are due to either man made or geographical boundaries such as fences, cliffs or water edges. In all cases the assumption is that for some reason the species can not wander across the boundary of their domain.

The functions  $y_1, y_2$  were given in equations (2.1) and (2.2) with interaction coefficients  $c_{ij}$  as in (2.5). Once again the fitness functions are as in the kinetic system (2.3), with  $f$  representing a pioneer species fitness function and  $g$  a climax species fitness function. The parameters  $D_1$  and  $D_2$  are the diffusion coefficients of the pioneer and climax species respectively.

In the first section the stability of the steady states of the kinetic system, which correspond to uniform steady states of (3.3), are examined. The next two sections deal with the analysis of a Turing bifurcation and the shape of the bifurcation diagram. In the last section we consider the Selgrade kinetic model introduced in Chapter 1 but with diffusion included.

## Stability of Uniform Steady States

In this section we will examine the stability of the uniform steady states of (3.3). Note that the steady state solutions of (2.3) correspond to uniform steady state solutions for (3.3)-(3.4). It is to our advantage to first nondimensionalize (3.3). In this regard let  $\hat{x} = \frac{x}{L}$  and  $\hat{t} = \frac{D_2}{L^2}t$ , in (3.3):

$$\begin{aligned}\frac{du}{d\hat{t}} &= du_{\hat{x}\hat{x}} + \gamma u f(y_1), \\ \frac{dv}{d\hat{t}} &= v_{\hat{x}\hat{x}} + \gamma v g(y_2),\end{aligned}\tag{3.5}$$

where  $d = \frac{D_1}{D_2}$  and  $\gamma = \frac{L^2}{D_2}$ , with boundary conditions given by

$$\begin{aligned}u_{\hat{x}}(0, \hat{t}) &= v_{\hat{x}}(0, \hat{t}) = 0, \\ u_{\hat{x}}(1, \hat{t}) &= v_{\hat{x}}(1, \hat{t}) = 0.\end{aligned}\tag{3.6}$$

For convenience the hat superscripts will be dropped.

Suppose  $(u^*, v^*)$  is an equilibrium point for the kinetic system (2.3). Then in view of the boundary conditions (3.6) we see that  $u = u^*$  and  $v = v^*$  is a trivial steady state solution to (3.5)-(3.6). To investigate the stability of this solution we linearize (3.5) about  $(u^*, v^*)$ . The linearized system is:

$$\begin{aligned}u_t &= du_{xx} + \gamma[u^* f'(y_1^*)c_{11} + f(y_1^*)](u - u^*) + \gamma[u^* f'(y_1^*)](v - v^*), \\ v_t &= v_{xx} + \gamma[v^* g'(y_2^*)](u - u^*) + \gamma[v^* g'(y_2^*)c_{22} + g(y_2^*)](v - v^*).\end{aligned}\tag{3.7}$$

Let  $\tilde{u} = u - u^*$  and  $\tilde{v} = v - v^*$  then (3.7) becomes,

$$\begin{aligned}\tilde{u}_t &= d\tilde{u}_{xx} + \gamma[u^* f'(y_1^*)c_{11} + f(y_1^*)]\tilde{u} + \gamma[u^* f'(y_1^*)]\tilde{v}, \\ \tilde{v}_t &= \tilde{v}_{xx} + \gamma[v^* g'(y_2^*)]\tilde{u} + \gamma[v^* g'(y_2^*)c_{22} + g(y_2^*)]\tilde{v}.\end{aligned}$$

This system can be written in the following form:

$$\begin{bmatrix} \tilde{u}_t \\ \tilde{v}_t \end{bmatrix} = \begin{bmatrix} d \frac{d^2}{dx^2} & 0 \\ 0 & \frac{d^2}{dx^2} \end{bmatrix} \begin{bmatrix} \tilde{u} \\ \tilde{v} \end{bmatrix} + \gamma DF(u^*, v^*) \begin{bmatrix} \tilde{u} \\ \tilde{v} \end{bmatrix}, \quad (3.8)$$

where  $DF(u^*, v^*)$  is the Jacobian of the vector field given in (2.3) evaluated at the point  $(u^*, v^*)$ . Since the problem (3.8) is linear we look for solutions in the form

$$\vec{u}(x, t) = \sum_{m=0}^{\infty} \vec{U}_m e^{\lambda_m t} \cos(m\pi x). \quad (3.9)$$

Substituting this form into (3.8) using the orthogonality of  $\{\cos(m\pi x)\}$  and canceling  $e^{\lambda_m t}$ , we obtain, for each  $m$

$$\lambda_m \vec{U}_m = [-(m\pi)^2 \mathbf{D} + \gamma DF(u^*, v^*)] \vec{U}_m \quad (3.10)$$

where  $\mathbf{D}$  is the diagonal matrix of diffusion coefficients. In order for this system to have a nontrivial solution it is necessary that

$$\det[\lambda_m \mathbf{I} + (m\pi)^2 \mathbf{D} - \gamma DF(u^*, v^*)] = 0. \quad (3.11)$$

If solutions to (3.11) give  $\text{Re}(\lambda_m) > 0$  for any  $m$ , then  $(u^*, v^*)$  is an unstable homogeneous steady state of the linearized diffusive system and therefore unstable in the nonlinear diffusive system [1], i.e. unstable to  $m^{\text{th}}$ -mode perturbations of the form  $\vec{v} \cos(m\pi x)$ . However if in (3.11),  $\text{Re}(\lambda) < 0$  for all  $m$ , then the equilibrium point is stable in both the linear and nonlinear diffusive system [28]. Notice that equation (3.11) becomes the eigenvalue equation for the kinetic system (2.3) when  $m = 0$ . If an equilibrium point was unstable in (2.3) then at  $m = 0$  the real part of an eigenvalue for (3.8) will be greater than zero, and thus the equilibrium point will also be unstable in the diffusive system (3.5). Since we are concerned with instability only due to the introduction of diffusion we are interested in linear instability of the equilibria that is solely spatially dependent. So, in the absence of diffusion we are concerned only with the stable equilibria of the kinetic system (2.3).

Table 1 gives the stability of the fixed points in the kinetic system. Recall that  $z_1$  is a zero of  $f$  and that  $w_1$  and  $w_2$  are zeros of  $g$ . Since  $p_0$  and  $p_1$  are unstable in all cases, the first point to consider in the diffusive system is  $p_2$  with  $f(\frac{w_2}{c_{22}}) < 0$ .  $DF(p_2)$  is given in equation (2.11). Equation (3.11) evaluated at this equilibrium point is

$$\begin{vmatrix} \lambda_m + d(m\pi)^2 - \gamma f(\frac{w_2}{c_{22}}) & 0 \\ -\gamma \frac{w_2}{c_{22}} g'(w_2) & \lambda_m + (m\pi)^2 - \gamma w_2 g'(w_2) \end{vmatrix} = 0.$$

Since  $f(\frac{w_2}{c_{22}}) < 0$  and  $g'(w_2) < 0$ , the eigenvalues are negative. Thus  $p_2$  remains stable in the diffusive system.

Next point to consider the equilibrium  $p_3$  with  $g(\frac{z_1}{c_{11}}) < 0$ . Equation (2.12) gives  $DF(p_3)$ . Equation (3.11) at this equilibrium point is

$$\begin{vmatrix} \lambda_m + d(m\pi)^2 - \gamma z_1 f'(z_1) & -\gamma \frac{z_1}{c_{11}} f'(z_1) \\ 0 & \lambda_m + (m\pi)^2 - \gamma g(\frac{z_1}{c_{11}}) \end{vmatrix} = 0.$$

Since  $f'(z_1) < 0$  and  $g(\frac{z_1}{c_{11}}) < 0$  the eigenvalues,  $\lambda_m$ , remain negative for all  $m$ , and therefore  $p_3$  is stable.

We consider the interior equilibrium points next. Refer to equation (2.13) for the Jacobian of the kinetic system at these equilibria. The eigenvalue equation is

$$\begin{vmatrix} \lambda_m + d(m\pi)^2 - \gamma c_{11} u_i^* f'(z_1) & -\gamma u_i^* f'(z_1) \\ -\gamma v_i^* g'(w_i) & \lambda_m + (m\pi)^2 - \gamma c_{22} v_i^* g'(w_i) \end{vmatrix} = 0$$

with eigenvalues

$$\begin{aligned} \lambda_{m\pm} &= -\frac{1}{2}[(d+1)(m\pi)^2 - \gamma \text{tr}(DF(q_i))] \\ &\pm \frac{1}{2} \sqrt{[(d+1)(m\pi)^2 - \gamma \text{tr}(DF(q_i))]^2 - 4h_m(d)} \end{aligned} \quad (3.12)$$

where

$$h_m(d) = d(m\pi)^4 - \gamma(dc_{22}v_i^*g'(w_i) + c_{11}u_i^*f'(z_1))(m\pi)^2 + \gamma^2 \det(DF(q_i)). \quad (3.13)$$

From Table 1 we see that  $q_2$  is stable when  $\det(C) > 0$ . Since  $f'(z_1) < 0$  and  $g'(w_2) < 0$ , equations (2.14) - (2.15) give us that  $\text{tr}(DF(q_2)) < 0$  and  $\det(DF(q_2)) > 0$ .

This implies that

$$-\frac{1}{2}[(d+1)(m\pi)^2 - \gamma \text{tr}(DF(q_2))] < 0$$

and from (3.13) that  $h_m(d) > 0$ , independent of  $m$  or  $d$ . Therefore  $\text{Re}(\lambda_{m\pm})$  are negative and  $q_2$  with  $\det(C) > 0$  is stable in the diffusive system.

The last point to consider is  $q_1$  with  $\det(C) < 0$  and  $\text{tr}(DF(q_1)) < 0$ . In this case  $\det(DF(q_1)) > 0$ , since  $g'(w_1) > 0$ . The above conditions give us that

$$-\frac{1}{2}[(d+1)(m\pi)^2 - \gamma \text{tr}(DF(q_1))] < 0 \quad (3.14)$$

but we see that  $h_m(d)$  may change sign. If  $h_m(d) < 0$  for some  $m$  we see from (3.11) that  $\text{Re}(\lambda_{m+})$  would be positive. This would cause a change in the stability of  $q_1$  due to the introduction of diffusion. We will examine this case further in the next section.

### Analytical Bifurcation Analysis

In this section we consider the steady state solution  $(u^*, v^*) \equiv q_1$ . Since we are interested with a diffusion driven instability we require that  $q_1$  is linearly stable in the absence on any spatial variation. We see from Table 1 that  $q_1$  is linearly stable in the kinetic system provided

$$\det(C) < 0 \text{ and } \text{tr}(DF(q_1)) < 0. \quad (3.15)$$

These conditions imply  $\det(DF(q_1)) > 0$  (see 2.15).

In the previous section we considered the full reaction diffusion system linearized about the steady states. Equation (3.12) gives the eigenvalues of the linearized system about  $q_1$ . For the equilibrium to become unstable to spatial disturbances, with  $d$  as the bifurcation parameter, we require  $\text{Re}(\lambda_m(d)) > 0$ , for some  $d$  and for some  $m \neq 0$ . With (3.15) satisfied we have from (3.14) that

$$-\frac{1}{2}[(d+1)(m\pi)^2 - \gamma \text{tr}(DF(q_1))] < 0.$$

However  $h_m(d)$  given in (3.13) may change sign. If  $h_m(d) < 0$ , then  $\text{Re}(\lambda_m(d)) > 0$  and  $q_1$  will have a diffusion driven instability.

First we consider the conditions under which  $h_m(d)$  will change sign as a function of  $d$ . If we rewrite (3.13) as follows:

$$h_m(d) = d[(m\pi)^4 - \gamma(m\pi)^2 c_{22} v_1^* g'(w_1)] + (\gamma^2 \det(DF(q_1)) - \gamma(m\pi)^2 c_{11} u_1^* f'(z_1)), \quad (3.16)$$

then we see that the second term in the sum is positive. Solving  $h_m(d) = 0$  for  $d$  gives us

$$d = d_m^* \equiv \frac{\gamma[(m\pi)^2 c_{11} u_1^* f'(z_1) - \gamma \det(DF(q_1))]}{(m\pi)^2 [(m\pi)^2 - \gamma c_{22} v_1^* g'(w_1)]}. \quad (3.17)$$

For (3.17) to be positive we need

$$(m\pi)^2 - \gamma c_{22} v_1^* g'(w_1) < 0. \quad (3.18)$$

Then for  $0 < d < d_m^*$ ,  $h_m(d) > 0$  and for  $d > d_m^* > 0$ ,  $h_m(d) < 0$  and at  $d = d_m^*$ ,  $h_m(d_m^*) = 0$ .

From equation (3.12) we see that  $\lambda_{m+}(d_m^*) = 0$ , for  $d < d_m^*$ ,  $\text{Re}(\lambda_{m+}(d)) < 0$  and for  $d > d_m^*$ ,  $\lambda_{m+}(d)$  is real and positive. Thus the  $m^{\text{th}}$  modal solution of  $q_1$  becomes unstable as  $d$  increases through  $d_m^*$ . Therefore we say that  $q_1$  becomes unstable due to the introduction of diffusion, or a Turing instability of  $q_1$  occurs at  $d = d_m^*$ . In the next section we will examine the bifurcating solutions and the bifurcation diagram for the first modal solution, i.e.  $m = 1$ . Also, from the sign of  $\lambda'_{1+}(d_1^*)$  and the shape of the bifurcation diagram we can determine the local stability of these bifurcating solutions [16].

### Local Bifurcation Analysis of Bifurcating Solutions near $q_1$

In this section we do a local bifurcation analysis about the uniform steady state solution  $q_1$  to determine the shape and direction of the bifurcation diagram with  $d$  as















































































































































